PWA FR-1276
8 MAR 1965

INVESTIGATION OF PRESSURE PREDICTION METHODS FOR RADIAL FLOW IMPELLERS

PHASE II

FINAL REPORT

Prepared Under Contract NAS8-5442

For

George C. Marshall Space Flight Center

Huntsville, Alabama

Written By: W. E. Young and H. F. Due

W. E. Young
Program Manager

H. F. Due
Senior Engineer

Approved By: C. D. Lingenfelter
C. D. Lingenfelter
Project Engineer

Pratt & Whitney Aircraft DIVISION OF UNITED AIRCRAFT CORPORATION

FLORIDA RESEARCH & DEVELOPMENT CENTER

FOREWORD

This report was prepared by Pratt & Whitney Aircraft's Florida Research and Development Center and presents a summary of the work conducted under the Phase II portion of Contract NAS8-5442, sponsored by the George C. Marshall Space Flight Center of the National Aeronautics and Space Administration, Huntsville, Alabama.

The work was administered under the technical direction of the Turbomachinery Unit of the Engine Systems Branch, Mr. Loren C. Gross, Chief, and covered the period from March 1964 to February 1965. A summary of the work conducted under the Phase I portion of the contract, covering the period from June 1963 to March 1964, was presented in PWA FR-952 "A Study of Pressure Prediction Methods for Radial Flow Impellers," dated 13 April 1964.

CONTENTS

ILLUSTRATIONS

LIST OF SYMBOLS

Symbol	Nomenclature	Units
C	Axial clearance between rotor and housing	Inches
C_m	Meridional velocity component or through flow velocity of fluid	ft/sec
f( )	Function of	
g	Acceleration due to gravity	ft/sec^2
H	Fluid static head	feet
K	Fluid angular velocity ratio, β/ω	Dimensionless
$\overline{\quad}_o$	Subscript, o, referring to the outer edge of disk or impeller	
P	Static pressure (Absolute)	psia
Δp	Peak to peak pressure pulse at blade passing frequency	psi
R	Impeller or disk radius	feet
Rey	Reynolds number of disk, $\omega R_o^2/\nu$	Dimensionless
S	Axial distance between housing and impeller surface, T + C	Inches
T	Blade height	Inches
u	Tangential impeller or disk velocity component	ft/sec
$\overline{\quad}_{1,2}$	Subscripts referring to radial location on disk	
β	Angular velocity of fluid	rad/sec
γ	Specific weight of fluid	lb/ft^3
ν	Kinematic viscosity	ft^2/sec
ϕ	Flow coefficient at impeller tip, C_m/u	Dimensionless
ω	Angular velocity of impeller	rad/sec
z	Clearance between tip blockage spacers and impeller or disk	Inches

ABSTRACT

This report presents the results of work performed under the second phase of Contract NAS8-5442, "Pressure Prediction Methods for Low Flow Radial Impellers." The two phases of the program consisted of (1) an experimental investigation of various factors affecting the distribution of pressure along radial-bladed or smooth rotating disks and (2) application of the test results to formulate an accurate method for predicting pressure distribution. The first phase was devoted entirely to incompressible flow conditions using water as the test fluid. The second phase extended the water flow tests to include rotor end effects, following which the entire test program was repeated with liquid hydrogen as the test fluid.

All tests were conducted in an apparatus in which the test fluid was directed radially outward along the front face of an 11-in. diameter rotor, into an annular collector, and then radially inward along the back face of the rotor to the rig discharge; thereby permitting investigation of both radially outward and inward flow conditions simultaneously. Pressure distribution was investigated over a range of rotor-to-housing axial clearances, flow coefficients and rotor speeds for the following rotor configurations:

Smooth disk with and without an inlet hub

24 blades, 0.125 inch high with and without rotor tip blockage

24 blades, 0.250 inch high

12 blades, 0.125 inch high

6 blades, 0.125 inch high.

Pressures at the inlet and discharge and at several radial stations, rotor speed, fluid inlet and discharge temperatures, and flow rate were measured and recorded for each test using a high speed data recording system. In addition, high-frequency blade-to-blade pressure data were measured and recorded on magnetic tape for the bladed-rotor tests. Data from these tests were used to develop regression equations with which pressure distribution for low flow radial impellers may be accurately predicted.

Fuller

SECTION I
INTRODUCTION

Inaccurately predicting the pressure distribution on high pressure turbopump impellers and the resulting axial thrust loads can result in severe consequences; realization of this led to the initiation of Contract NAS8-5442, "Investigation of Pressure Prediction Methods for Low Flow Radial Impellers." Existing methods for predicting pressure distribution on the low-flow back face of centrifugal pumps resulted in 10 to 15% inaccuracies in the predicted axial thrust loads on high pressure hydrogen and oxygen turbopumps tested at FRDC. Errors of this magnitude, in applications where the pressure-area product is high, can produce an excessive axial thrust unbalance which may lead to pump failure; this occurred in the early high pressure liquid hydrogen turbopump tests.

The purpose of the program under Contract NAS8-5442 was to determine the effects of rotor configuration and operating conditions on pressure distribution and to formulate a more accurate method of predicting pressure distribution. The experimental test program included investigation of both smooth and bladed disks for radially inward and outward flow conditions at various disk-to-housing clearances, flow rates and rotor speeds. The effect of blade height and the number of blades was also investigated in the bladed disk tests. In the Phase I portion of the contract the effect on pressure distribution of these various parameters was established for an incompressible fluid using water as the test fluid.† In the Phase II portion (the results of which are reported herein) additional water tests were conducted to determine the effect of changes in the impeller inlet and discharge geometry by the addition of an inlet hub on the smooth disk and by blockage at the tip of the bladed disk. All of the tests previously conducted with water were then repeated using liquid hydrogen as the test fluid.

Experimental test data were obtained for smooth disks with axial clearances from 0.024 to 0.156 inch, and for bladed disks with 24, 12, and 6 blades and blade heights of 0.125 and 0.250 inch at blade-to-housing clearances of 0.065 to 0.125 inch. The end effect tests provided data at

† PWA FR-952, "A Study of Pressure Prediction Methods for Radial Flow Impellers," Final Report, 13 April 1964

inlet diameter-to-hub diameter ratios of 1.33 and 2.0 and tip blockage clearances of 0.050, 0.100 and 0.150 inch. These data were used to develop regression equations from which pressure distribution can be determined for a given pump configuration and operating condition.

SECTION II
EXPERIMENTAL EQUIPMENT

The test apparatus used in the study (figure II-1) is described in the Phase I final report;† it was adapted for use with liquid hydrogen by replacing the bearings and seals in the main test rig and by adding a liquid hydrogen flow loop to the test facility. The apparatus consists of three large stainless steel housings and a smaller fourth housing to adapt it to the facility drive unit. The rotor (bladed or unbladed) was suspending using two ball bearings cooled with the discharge fluid of the apparatus. Two seal compartments were employed to purge the leakage from the bearing compartment while testing with liquid hydrogen and also to adjust the thrust loads on the bearings by varying the nitrogen purge gas flow into the front compartment. The apparatus was designed to run at tip pressures to 1000 psia and rotating speeds to 20,000 rpm. Ring spacers were provided between the front and rear housings to adjust the axial clearance. Two of the rotors used to provide different rotor configurations are shown in figure II-2. Nine basic configurations were considered; smooth or unbladed disk at three clearances, 0.125 inch blade height disk at three clearances, and 0.250 inch blade height disk at three clearances. In addition to the basic test configurations, several end effect configurations were investigated; two sizes of hubs located at the inlet portion of the smooth or unbladed disk and three tip blockage rings to overhang the tip of the bladed disk to give different impeller tip-to-blockage ring clearances. The facility used for the Phase II investigation was modified slightly from that described in the Phase I final report to permit testing with liquid hydrogen. A schematic of the flow loop for the water tests is shown in figure II-3. A 5000 gal portable tank was used as the demineralized water source. Flow, supplied to the test apparatus by a centrifugal pump, was controlled by a remotely operated pneumatic valve located downstream of the test rig. The test apparatus was driven by a constant speed (1500 hp) motor through a Dynamatic clutch and gearbox with a maximum output speed of 35,000 rpm. Speed was controlled to within 1% of the set value.

---

† Ibid

The flow system, modified for testing with liquid hydrogen, is schematically shown in figure II-4. The open system was employed because of the tendency of liquid hydrogen to absorb heat and flash to a vapor. Liquid hydrogen was supplied by pressurizing a 7000 gal, vacuum jacketed, portable dewar to approximately 90 psig, and allowing the hydrogen to flow through a vacuum jacketed inlet line to the test apparatus, from which it was discharged to a burn stack and allowed to burn in the atmosphere. The flow rate was controlled by a pneumatic operated control valve located immediately downstream of the apparatus. A photograph of the liquid hydrogen flow system is shown in figure II-5. The motor drive system was enclosed in a sheet metal building which was pressurized (as a safety precaution) while testing with liquid hydrogen.

All tests were conducted remotely from a control room adjacent to the flow system. The dewar liquid level, dewar pressure, flow rate, inlet temperature and pressure, discharge temperature and pressure, purge cavity pressure, and rotor speed were displayed in the control room for monitoring during each test. These items plus all of the radial pressures and temperatures located on the apparatus front and rear housings were recorded on digital tape using an automatic data recording system. Static pressure taps were close coupled with Tabor pressure transducers Model 217 SA; radial fluid temperatures were measured using copper-constantan thermocouples. Liquid hydrogen temperatures were measured using Rosemont resistance type thermometers, Model No. 150E and 157T (within 0.25°R accuracy). Transient pressures generated by the rotating blades passing a transducer were recorded on a frequency-modulated tape unit using Kistler Model 601A quartz crystal pressure transducers close coupled with the Model 624 adapter. The tape was analyzed after each test with a panoramic wave analyzer having a Polaroid attachment.

A torque measuring device, consisting of a torque sensor shaft mounted in the drive unit and a magnetic pickup located at each end of the shaft, was provided between the gearbox drive unit and the test apparatus. The angle of twist of the shaft (proportional to the torque applied by the rotor in the test apparatus) was measured by the change in phase angle at each end of the torque sensor shaft. The output was displayed in the control room and recorded by the automatic data recording system on digital

tape. The digital recording system was capable of scanning and recording each channel every 0.014 sec (approximately). The data tape was reduced using the IBM 7090 computer.

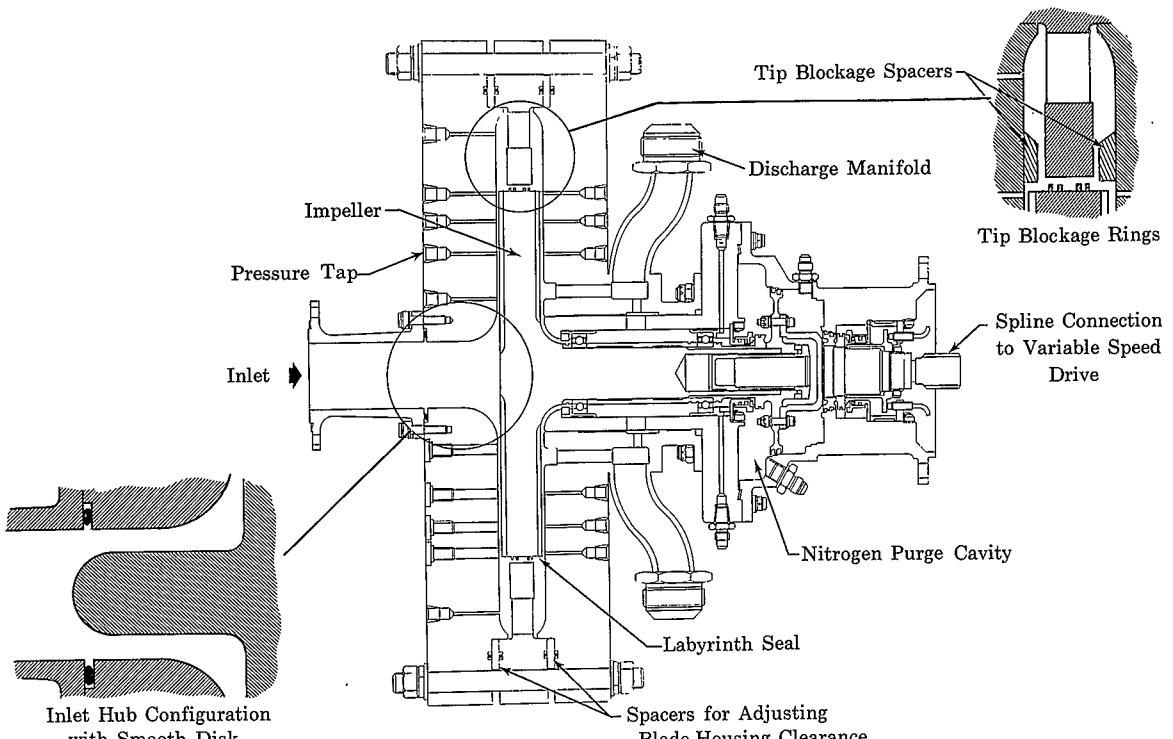

Figure II-1. Pressure Distribution Test Apparatus

FD 10984

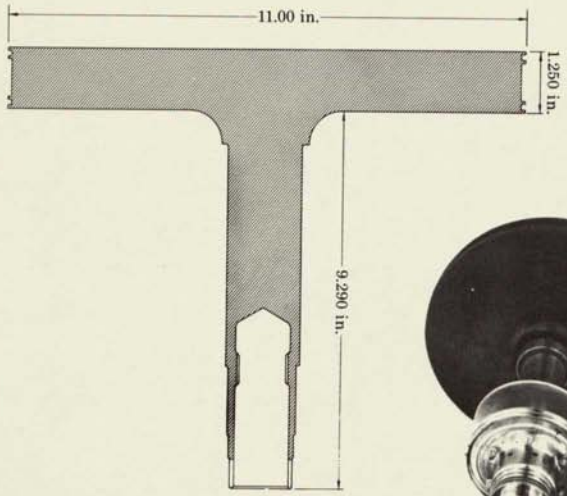

Shaft dia 1.575 in.

Sketch of Unbladed Rotor

Assembly of Unbladed Rotor

Front and Rear View of 0.250-in. Bladed Rotor

Figure II-2. View of Test Rotors

FD 7566C

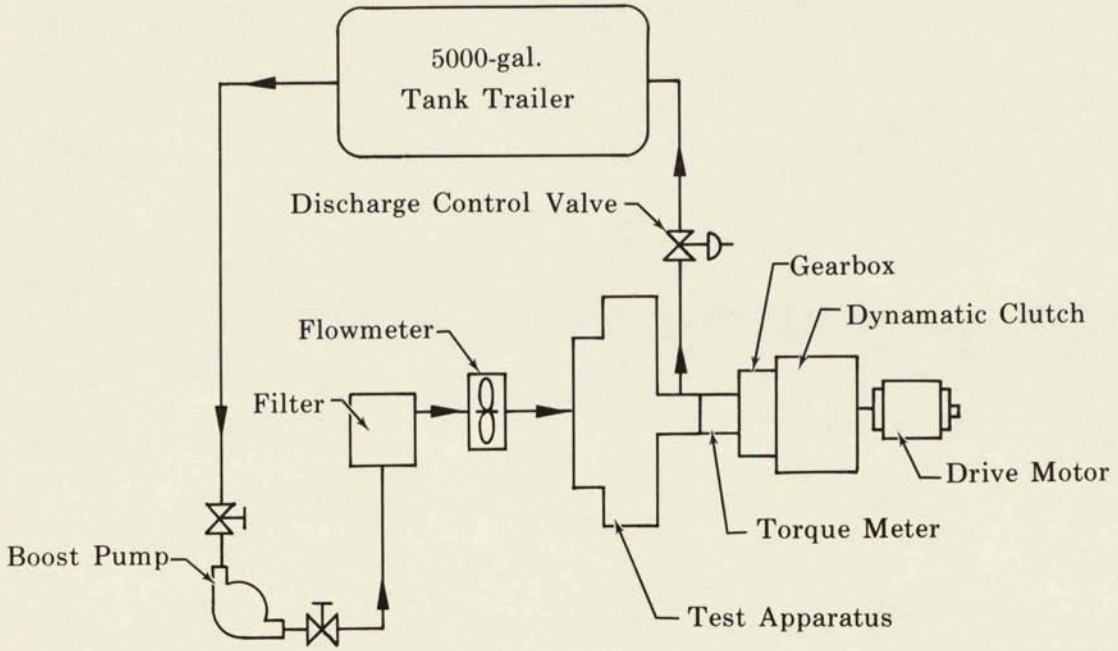

Figure II-3. Schematic of Flow Loop for Water Tests

FD 11007

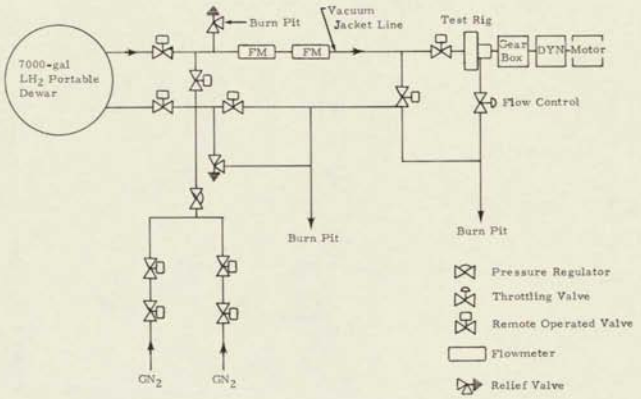

Figure II-4. Schematic of Flow Loop for Liquid Hydrogen Tests

FD 10989

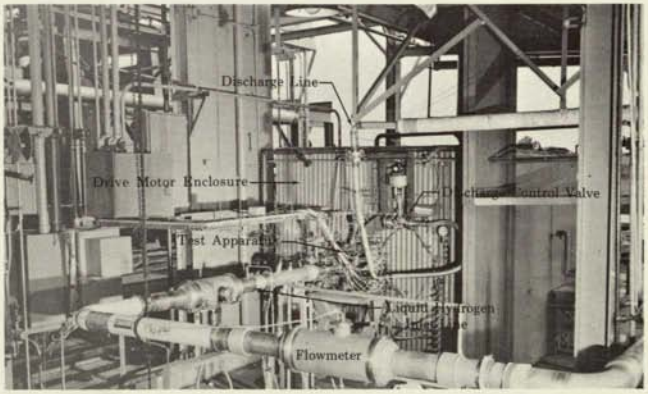

Figure II-5. View of Test Stand Showing Test Apparatus Installation

FD 10993

SECTION III
EXPERIMENTAL PROCEDURES

The pressure distribution test apparatus was reassembled for each disk configuration tested, at which time the fits and tolerances of the various components were checked and worn or damaged parts replaced. New ball bearings were installed in the apparatus for each assembly and runouts on the rotating assembly were measured at various stages during the build. The axial and radial runout of the disk were generally less than 0.0015 in. at the outer radius of the disk. The axial clearance between the disk and housing was adjusted so that the front clearance was equal to the rear clearance to within 0.001 in.

To facilitate clearance changes while the test apparatus was installed in the test stand, most of the instrumentation was attached to the housings and leak checked during assembly.

Duration for each test was approximately 20 minutes, and about nine data points were recorded. Data points were taken at selected speeds and flow rates during a period of several minutes of steady-state running. Approximately ten seconds of high speed data was recorded (about one scan every 0.015 sec) for each data point.

Liquid hydrogen test procedures were almost identical to the water test procedures; however, in the former, the test time was shortened to conserve hydrogen. Because of inherently different physical and thermodynamic properties, the speed-flow limits were quite different for the two fluids. The drive system torque limits (approximately 200 ft-lb) restricted the water tests to speeds to 5000 rpm and the supply pump output restricted flow rates to 50 gpm; however, this combination satisfactorily covered the range of flow coefficients required. Heat addition (due to fluid friction) limited the maximum speed in the hydrogen tests to approximately 14,000 rpm because of the tendency of the hydrogen to boil. The maximum flow rate was restricted to approximately 300 gpm by the pressure limit (90 psig) on the supply dewar. At the upper speed range the minimum flow rate was critical because of the energy input to the fluid. Cavitation within the test apparatus was noted when operating outside of these speed and flow limits. These limitations restricted the liquid hydrogen test program to flow coefficients between 0.015 and 0.030 (calculated at the

disk tip); however, the data obtained is believed to be sufficient to correlate the variables involved.

At the completion of each test, the data tape was reduced on the IBM 7090 and the results analyzed.

SECTION IV
RESULTS OF EXPERIMENTAL PROGRAM

A. GENERAL

The results of the experimental program consisted of the various radial pressure distributions reduced and classified according to flow coefficient, speed and type of geometric configuration, the transient blade-to-blade pressure recording, and the torque data. A summary of the data from the test runs of Phase II is presented in tables IV-1 and IV-2 for the water tests and the liquid hydrogen tests respectively.

B. RADIAL STATIC PRESSURE DISTRIBUTION

The radial static pressure measurements were converted to head rise and plotted against radius squared for each test. The slope of the head-radius squared curves describes the vortex mode existing on the surface of the disk. For example, a head-radius squared curve that is a straight line represents a pure forced vortex, whereas one which is curved signifies a free vortex. A pure forced vortex curve can be described using a single equation for predicting the head distribution.

$$\Delta H = \left(\frac{K^2 \omega^2}{2g}\right)\left(R_2^2 - R_1^2\right) \tag{1}$$

The term K is defined as the fluid angular velocity ratio

$$K = \beta/\omega \tag{2}$$

If K varies with the disk radius a forced vortex does not exist and the head rise prediction equation must contain the $K = f(R^2)$ term, which must be integrated over the disk radius. In this study a finite difference method type of integration was used. The head-radius squared curve was divided into small increments, each of which approximated a straight line and a K value was computed for each increment. A compilation of K values with the other variables involved were input to a multiple regression analysis program on the IBM 7090 and an equation for K was produced. Equations for K for all of the configurations tested are presented in Section V.

The ideal head rise is achieved if K is equal to unity. The maximum value that can possibly be attained through the various changes to the rotor is therefore unity.

1. Smooth Disk with Inlet Hub in Water (Table IV-1, Tests 1 and 2)

Two tests were conducted on the smooth disk with an inlet hub, one with an inlet diameter to hub diameter ratio of 1.33 and the other 2.0. This configuration is similar to the physical case of the back face of a pump impeller where the flow is radially outward and where, in effect, the impeller shaft is simulated by the hub. This is shown as an insert in figure II-1.

The $\Delta H\text{-}R^2$ curves obtained are shown in figure IV-1. There was no appreciable difference in the results obtained between the two diameter hubs used. Comparison of the head rise values from the smooth disk tests without a hub in Phase I shows that there is a decrease in head rise with the addition of the hub. Calculation of K from the $\Delta H\text{-}R^2$ curves revealed a major discrepancy between the data from these tests and the K curves for a smooth disk without hub generated in Phase I. Figure IV-2 shows the K values calculated from the smooth disk tests in Phase I plotted against flow coefficient for the clearances tested. Based on the findings of other investigators† who have found that the fluid velocity ratio at shutoff flow for clearances below 0.200 in. between a stationary housing and a smooth rotating disk is approximately equal to 0.5, the curves in figure IV-2 were projected to a common apex at approximately K = 0.5 for $\phi = 0$ even though the data from two of the tests (at C = 0.094 and 0.113) were not in close agreement with the curves. This was attributed to the fact that these tests were conducted without a positive control of the shaft axial position and the rotor-to-housing clearance, i.e., the shaft position was monitored with an inductance type proximity indicator and controlled by a balance piston that could be loaded in either direction to maintain the required clearance. The inaccuracy of this system, due primarily to the effect of temperature changes on the proximity probes, made the actual rotor clearances questionable.

For the third smooth disk test (C = 0.040) and all subsequent tests an improved ball bearing was used that could withstand the rotor axial thrust load and provide positive location of the shaft within ± 0.001 inch. The slope of the K curves from the hub tests run in Phase II did

†Daily, J.W. and R.E. Nece, "Chamber Dimension Effects on Induced Flow and Frictional Resistance of Enclosed Rotating Disks," ASME Transactions, Journal of Basic Engineering, March 1960, pp 217-232.

not agree with the curves shown in figure IV-2. Therefore, a baseline test on the smooth disk without a hub was conducted to investigate this discrepancy. The K curve from this test, which was run at a clearance of 0.138 in., is shown superimposed on figure IV-2. The slope of the K curve from this test agreed closely with that of the hub test and, as can be seen in figure IV-2, is the same as the slope of the curve from the test at C = 0.040 in Phase I. This subject is discussed further in Section VI (Conclusions).

2. Bladed Disk with Tip Blockage in Water (Table IV-1, Tests 3, 4, and 5)

Three tests were performed using a 0.125 in. high, 24-blade disk with different values of tip blockage clearance. Tip blockage is defined as the overhang of the housing on the back face of an actual impeller. Tip blockage as applied to the test apparatus is shown in an insert in figure II-1. Figure IV 3(a) shows the tip blockage radial head distribution curves for outward flow with water. Note that with the addition of the tip blockage the curve tends toward a straight line. The net effect of tip blockage on overall head rise across the disk was found to be slight. However, there is a significant change in head rise distribution due to the change in slope of the curve. There was a smaller change in the head distribution for the inward flow case as shown in figure IV-3(b).

3. Smooth Disk in Liquid Hydrogen (Table IV-2, Tests 1, 2, and 3)

Three tests were conducted using a smooth disk at various clearances to determine the effect of the clearance change on pressure distribution with liquid hydrogen as the test fluid. A typical head distribution curve is shown in figure IV-4(a) for the outward flow case. The inward flow condition is shown in figure IV-4(b). Generally the ΔH-R^2 curves for the smooth disk, outward flow condition were straight lines. At the lower value of clearance the temperature rise in the hydrogen was large enough to have a substantial effect on the density and in turn the head distribution; however, an approximation to a straight line was made and the data was analyzed in the same manner as in the larger clearances.

In analyzing the test data from all of the liquid hydrogen tests it was necessary to assume a temperature variation along the radius of the disk from the inlet to the tip with the end points given by the Rosemont temperature probes. This assumption was necessary because the physical

size of the flow passage made it impossible to immerse a probe along the face of the disk. A temperature rise varying linearly with radius squared was assumed and used for determining the radial density variation and therefore the conversion of radial pressure distribution to head distribution.

For the inward flow condition with liquid hydrogen the head drop curve was not a straight line as was the case for outward flow. This is similar to what was observed with the inward flow of water on a smooth disk.

In Phase I, attempts made to analyze the smooth disk inward flow data were complicated by the fact that the vortex mode was dependent on radius ratio as well as clearance and flow coefficient. However, by deriving a K value as a function of the influencing variables it was possible to describe the pressure distribution using the simple forced vortex equation.

4. Bladed Disk in Liquid Hydrogen (Table IV-2, Tests 5, 7, 8, 11, 15 and 16)

Two disks with 24 blades, 0.125 in. and 0.250 in. high were tested using three different clearance values for each to provide the data for determining a pressure prediction method for a bladed disk. Two additional tests were conducted with the 0.125 in. high bladed disk with 12 and 6 blades to evaluate the effect of number of blades. Typical head distribution curves are shown in figure IV-4(c) and (d) for the 0.125 in. blade and (e) and (f) for the 0.250 in. blade.

Most of the ΔH-R^2 curves for the outward flow of liquid hydrogen on a bladed disk plotted as straight lines for all values of clearance, blade heights and different number of blades. Also, the K value calculated from the ΔH-R^2 curves revealed that K was unity for all configurations of the bladed disk within the accuracy of the test results. Figure IV-5 shows some of the reduced data plotted as K vs $(R/R_o)^2$.

The inward flow condition yielded a head distribution curve similar to all previous inward flow cases (that is, a curved ΔH-R^2 line). The inward flow K appeared to be affected by clearance, radial span, flow coefficient and blade height, and these variables were used to determine K from the regression analysis.

5. Smooth Disk with Inlet Hub in Liquid Hydrogen (Table IV-2, Test 4)

Since the addition of an inlet hub was found to have an effect on the head rise on a smooth disk with outward flow in water, the same test was made using hydrogen as the test fluid to determine if a similar effect existed. The results of the tests with hydrogen showed an effect contrary to the effect found with water. In water, the addition of the inlet hub tended to decrease the overall head rise; however, with liquid hydrogen the head rise was increased by the addition of an inlet hub. This difference in results is discussed further in Section V. Figure IV-6(a) shows the head distribution for a smooth disk with inlet hub in liquid hydrogen.

6. Bladed Disk with Tip Blockage in Liquid Hydrogen (Table IV-2, Tests 9, 10, and 12)

The head distribution curves obtained for the tip blockage configuration tests are shown in figure IV-7(a) for outward flow and (b) for inward flow. It can be generally stated that the tip blockage did not have a major effect on the shape of the ΔH-R^2 curves since with or without tip blockage the lines were straight for outward flow. But the curves of figure IV-7(a) do show an increase in head rise for tip blockage clearance values of 0.050 and 0.100 in.; however, K values calculated from these curves were greater than unity, an impossibility that casts suspicion on the temperature distribution assumed in calculating density and, in turn, head rise. The temperature rise from the inlet to the impeller tip discharge annulus for the tests at the lower tip blockage clearance values showed a marked increase over the tests without tip blockage. Because the assumption of a linear temperature rise with radius squared for these tests results in K values greater than unity, it becomes apparent that the observed temperature rise is not generated entirely across the face of the disk. This leads to the conclusion that part of the temperature rise is produced by the pumping action or fluid friction between the tip of disk and the tip blockage ring at lower values of tip clearance and that the temperature rise through this passage increases as clearance decreases. A similar question exists on the temperature rise for the inward flowing condition for which data is presented in figure IV-7(b). If the K value for outward flow is assumed equal to unity then a temperature

rise through the passage between the tip of the disk and the tip blockage ring can be estimated. Application of the same temperature correction to inward flow results in K values that are nearly the same as the tests without tip blockage. These results led to the assumption that tip blockage has no measurable effect on K for either outward or inward flow.

7. Bladed Disk with Varying Number of Blades in Liquid Hydrogen (Table IV-2, Tests 13 and 14)

Typical head distribution curves for the tests performed with varying number of blades are shown in figure IV-8. It should be noted that even though the curves show a decrease of head rise with decreasing number of blades for both the outward and the inward flow condition the average K values for these tests is equal to unity.

As mentioned previously in discussing the results of the liquid hydrogen tests, the temperature rise of the liquid flowing along the disk has a significant effect on the pressure rise and therefore the calculated head rise. Figure IV-9 shows a typical temperature rise vs flow coefficient for a bladed disk. A comparison of the data from all configurations at different speeds and flow coefficients showed that the temperature rise values obtained were not consistent from test to test. Figure IV-10 shows a range of temperature rise vs rotational speed for the bladed disk. There was too much scatter in the data to obtain a correlation between temperature rise and flow coefficient, and/or geometry effects. The range shown is believed to be representative of the values that would occur if operating within the limits described in Section V.

C. BLADE-TO-BLADE PRESSURE OSCILLATIONS

The pressure pulse generated by a blade sweeping past a high response pressure transducer (described in Section II) were recorded on magnetic tape during test. These tapes were analyzed on a multi-channel wave analyzer, and photographs taken of typical test points are shown in figure IV-11. Each photograph is a display of the peak-to-peak pressure amplitudes at the frequency of the complex wave generated by the passing blade. Several pressure pulses appear on each photograph. The pulse of primary interest in this study occurs at the frequency of the passing blade. At higher frequencies harmonics appear. With the 24-blade rotor the amplitudes of the harmonics were quite low; however, for the 12 and 6

blade disk the higher harmonics were quite distinct. At the disk rotating frequency pulses were also visible and were probably caused by a slight axial runout of the disk. A blade pressure loading parameter was calculated from the data and plotted against radius ratio squared and is shown in figure IV-12. The blade pressure loading parameter was defined as the peak-to-peak pressure pulse at the blade passing frequency divided by the local average static pressure (or $\Delta p/P$). There did not appear to be a readily predictable trend from the data plotted but the results with liquid hydrogen were clearly different from those with water. The $\Delta p/P$ for the water tests in Phase I were also very erratic but the data indicated a constant value of 0.075 independent of speed, clearance, radius ratio and number of blades.

D. TORQUE DATA

The energy input to the rotating disk was obtained using the torque measuring apparatus described in Section II of this report. The torque measurements are used to calculate the moment coefficients, which assist in the prediction of disk friction for smooth disks and required driving power for bladed disks.

The torque data taken during the water tests in Phase II was found to be erratic and not consistent from test point to test point. A complete calibration of the torque measuring unit did not reveal the cause of the discrepancies in the measurements. The same system was used for the liquid hydrogen tests and again the torque data was found to be inconsistent and therefore is considered invalid.

Table IV-1. Summary of Test Data for Phase II (Water)

Test No.	Axial Clearance, (in.)	Blade Height, (in.)	Shaft Speed, rpm	Flow Rate, gpm	Flow Coeff.	Reynolds No. (10^6)	Remarks
1.01	0.080	0.00	2036	31.3	0.0388	4.92	Smooth Disk with
1.02	0.080	0.00	2014	19.5	0.02442	4.88	Hub at Inlet:
1.03	0.080	0.00	2069	3.2	0.0039	5.18	Inlet Diameter/
1.04	0.080	0.00	3005	30.7	0.02577	7.12	Hub Diameter =
1.05	0.080	0.00	3046	19.5	0.01615	7.33	1.33
1.06	0.080	0.00	3035	3.1	0.00260	7.49	
1.07	0.080	0.00	4002	32.4	0.02043	9.91	
1.08	0.080	0.00	4001	19.1	0.01204	10.1	
1.09	0.080	0.00	4021	3.1	0.00198	11.4	
2.01	0.080	0.00	1984	29.5	0.03751	4.61	Smooth Disk with
2.02	0.080	0.00	2000	20.4	0.02573	4.66	Hub at Inlet:
2.03	0.080	0.00	2046	3.35	0.00419	4.88	Inlet Diameter/
2.04	0.080	0.00	3022	31.7	0.02646	7.11	Hub Diameter =
2.05	0.080	0.00	3006	19.8	0.01661	7.14	2.00
2.06	0.080	0.00	3054	3.2	0.00264	7.90	
2.07	0.080	0.00	4197	30.2	0.01816	10.1	
2.08	0.080	0.00	4177	21.5	0.01299	10.2	
2.09	0.080	0.00	4212	3.2	0.00191	12.0	
3.01	0.065	0.1250	2005	29.8	0.01616	5.14	Bladed Disk,
3.02	0.065	0.1250	2028	18.7	0.01002	5.22	24 Blades
3.03	0.065	0.1250	2055	2.7	0.00142	5.51	Tip Blockage
3.04	0.065	0.1250	3117	33.7	0.01175	8.16	Z = 0.100 in.
3.05	0.065	0.1250	3157	20.7	0.00713	8.42	
3.06	0.065	0.1250	3200	2.7	0.00091	10.6	
3.07	0.065	0.1250	4184	33.1	0.00860	11.3	
3.08	0.065	0.1250	4190	24.7	0.00641	11.6	
3.09	0.065	0.1250	4226	2.8	0.00072	14.4	
4.01	0.065	0.1250	2043	31.2	0.01660	5.16	Bladed Disk,
4.02	0.065	0.1250	2079	20.6	0.01077	5.28	24 Blades
4.03	0.065	0.1250	2061	2.1	0.00110	5.50	Tip Blockage
4.04	0.065	0.1250	Incomplete Data				Z = 0.050 in.
4.05	0.065	0.1250	3052	22.0	0.00784	7.90	
4.06	0.065	0.1250	3087	2.5	0.00088	8.85	
4.07	0.065	0.1250	4106	36.4	0.00964	10.7	
4.08	0.065	0.1250	4171	26.6	0.00693	11.1	
4.09	0.065	0.1250	4215	2.6	0.00067	14.3	

Table IV-1. Summary of Test Data for Phase II (Water) (Continued)

Test No.	Axial Clearance, (in.)	Blade Height, (in.)	Shaft Speed, rpm	Flow Rate, gpm	Flow Coeff.	Reynolds No. (10^6)	Remarks
5.01	0.065	0.1250	2054	31.2	0.01651	5.03	Bladed Disk,
5.02	0.065	0.1250	2100	20.1	0.01040	5.18	24 Blades
5.03	0.065	0.1250	2122	2.3	0.00117	5.47	Tip Blockage
5.04	0.065	0.1250	3056	35.9	0.01277	7.59	Z = 0.150 in.
5.05	0.065	0.1250	3332	23.0	0.00750	8.44	
5.06	0.065	0.1250	3363	2.3	0.00074	9.62	
5.07	0.065	0.1250	4058	30.8	0.00825	10.5	
5.08	0.065	0.1250	4071	23.1	0.00617	10.8	
5.09	0.065	0.1250	4115	2.3	0.00060	14.3	
6.01	0.065	0.1250	1987	30.4	0.01663	4.95	Bladed Disk,
6.02	0.065	0.1250	2002	20.4	0.01108	5.07	24 Blades
6.03	0.065	0.1250	2005	2.4	0.00130	5.46	
6.04	0.065	0.1250	3200	32.9	0.01118	8.42	
6.05	0.065	0.1250	3181	23.3	0.00797	8.64	
6.06	0.065	0.1250	3196	5.1	0.00173	10.5	
6.07	0.065	0.1250	4149	34.1	0.00894	11.7	
6.08	0.065	0.1250	4095	21.8	0.00579	12.6	
6.09	0.065	0.1250	4102	2.6	0.00069	16.9	
7.01	0.138	0.00	2998	30.9	0.01496	7.57	Smooth Disk
7.02	0.138	0.00	3050	21.2	0.01009	7.79	
7.03	0.138	0.00	2970	1.8	0.00087	8.86	
7.04	0.138	0.00	4297	28.8	0.00973	11.2	
7.05	0.138	0.00	3943	24.2	0.00891	10.3	
7.06	0.138	0.00	4267	2.0	0.00068	14.2	
7.07	0.138	0.00	4928	30.6	0.00902	13.2	
7.08	0.138	0.00	5010	20.3	0.00588	14.1	
7.09	0.138	0.00	5185	1.9	0.00053	19.3	

Table IV-2. Summary of Test Data for Phase II (LH_2)

Test No.	Axial Clearance, in.	Blade Height, in.	Shaft Speed, rpm	Flow Rate, gpm	Flow Coeff.	Reynolds No. (10^6)	Remarks
1.01	0.138	0	10772	26.6	0.004	87.2	Smooth Disk
1.02	0.138	0	10639	69.9	0.0105	87.2	
1.03	0.138	0	10021	85.2	0.0135	82.5	
1.04	0.138	0	9973	91.9	0.0145	83.0	
1.05	0.138	0	13061	61.6	0.0077	104.7	
1.06	0.138	0	13377	88.5	0.0108	107.4	
1.07	0.138	0	12778	91.5	0.0117	102.7	
1.08	0.138	0	15250	75.0	0.0081	123.0	
2.01	0.065	0	10402	42.3	0.0136	83.5	Smooth Disk
2.02	0.065	0	10088	59.8	0.0197	82.2	
2.03	0.065	0	9988	77.6	0.0255	82.4	
2.04	0.065	0	12017	49.1	0.0137	95.6	
2.05	0.065	0	11911	73.9	0.0210	95.7	
2.06	0.065	0	11970	87.9	0.0247	97.0	
2.07	0.065	0	13948	93.8	0.0231	110.8	
2.08	0.065	0	14022	74.4	0.0183	110.6	
2.09	0.065	0	13963	66.3	0.0164	109.5	
3.01	0.024	0	10022	134.5	0.1230	82.8	
3.02	0.024	0	10042	76.5	0.0725	79.9	
3.03	0.024	0	10110	56.0	0.0544	78.0	Smooth Disk
3.04	0.024	0	10095	37.7	0.0368	77.6	
3.05	0.024	0	12062	125.5	0.0991	95.9	
3.06	0.024	0	12058	110.4	0.0877	95.3	
3.07	0.024	0	12146	83.6	0.0678	93.4	
3.08	0.024	0	14158	122.3	0.0854	108.4	
3.09	0.024	0	14179	100.7	0.0713	107.0	
3.10	0.024	0	14126	80.6	0.0576	106.0	
4.01	0.065	0	10050	194.2	0.0630	85.1	
4.02	0.065	0	9975	120.0	0.0400	80.3	
4.03	0.065	0	10023	74.8	0.0257	77.2	Smooth Disk with Hub at Inlet
4.04	0.065	0	11867	95.3	0.0279	90.8	
4.05	0.065	0	12030	152.5	0.0429	97.3	Inlet Diameter/ Hub Diameter 2/1
4.06	0.065	0	11978	195.6	0.0539	100.4	
4.07	0.065	0	13787	164.6	0.0410	110.3	
4.08	0.065	0	14085	127.7	0.0322	107.9	
4.09	0.065	0	13851	90.8	0.0233	104.5	
5.01	0.140	0.250	4532	160.5	0.0195	38.9	Bladed Disk, 24 Blades
5.02	0.140	0.250	4531	142.7	0.0174	38.8	
5.03	0.140	0.250	4500	100.8	0.0126	37.3	
5.04	0.140	0.250	5902	210.7	0.0199	50.6	
5.05	0.140	0.250	5870	149.8	0.0146	48.3	

Table IV-2. Summary of Test Data for Phase II (LH_2) Continued

Test No.	Axial Clearance, in.	Blade Height, in.	Shaft Speed, rpm	Flow Rate, gpm	Flow Coeff.	Reynolds No. (10^6)	Remarks
5.06	0.140	0.250	5883	130.4	0.0128	47.7	
5.07	0.140	0.250	5873	117.9	0.0116	47.5	
5.08	0.140	0.250	6452	191.4	0.0167	54.3	
5.09	0.140	0.250	6425	130.7	0.0118	51.9	
5.10	0.140	0.250	9060	291.7	0.0190	74.3	Bladed Disk, 24 Blades
5.11	0.140	0.250	10460	246.9	0.0153	78.2	
5.12	0.140	0.250	10100	228.1	0.0146	74.9	
5.13	0.140	0.250	9060	177.3	0.0128	66.7	
6.01	0.065	0.250	Failure of tip kiel probe aborted run and caused severe damage to rear blades.				
7.01	0.035	0.125	9329	321.5	0.0458	83.1	Bladed Disk, 24 Blades
7.02	0.035	0.125	9343	191.8	0.0279	80.6	
7.03	0.035	0.125	10306	238.2	0.0315	89.5	
7.04	0.035	0.125	10301	188.0	0.0235	87.1	
7.05	0.035	0.125	11420	238.1	0.0292	95.8	
7.06	0.035	0.125	12309	286.7	0.0324	105.0	
7.07	0.035	0.125	11929	235.4	0.0279	98.9	
7.08	0.035	0.125	12294	229.1	0.0267	101.2	
7.09	0.035	0.125	12275	224.4	0.0262	100.3	
7.10	0.035	0.125	12783	177.3	0.0214	96.6	
7.11	0.035	0.125	13449	174.6	0.0208	97.8	
7.12	0.035	0.125	14141	234.6	0.0253	109.5	
8.01	0.073	0.125	9249	305.9	0.0361	80.5	Bladed Disk, 24 Blades
8.02	0.073	0.125	9186	235.2	0.0285	78.0	
8.03	0.073	0.125	9200	133.7	0.0180	68.3	
8.04	0.073	0.125	11274	281.7	0.0284	94.1	
8.05	0.073	0.125	11202	236.9	0.0246	90.9	
8.06	0.073	0.125	11204	158.9	0.0181	82.0	
8.07	0.073	0.125	13306	284.0	0.0257	104.7	
8.08	0.073	0.125	13283	241.4	0.0226	100.9	
8.09	0.073	0.125	13215	182.4	0.0185	92.5	
8.10	0.073	0.125	14405	237.6	0.0214	104.5	
8.11	0.073	0.125	15578	246.5	0.0215	108.6	
8.12	0.073	0.125	Flow Oscillation				
9.01	0.073	0.125	8908	247.5	0.0351	66.9	Bladed Disk, 24 Blades
9.02	0.073	0.125	8903	168.7	0.0246	64.3	
9.03	0.073	0.125	8918	83.5	0.0135	56.7	Tip Blockage Z = 0.050 in.
9.04	0.073	0.125	10895	248.8	0.0287	81.9	
9.05	0.073	0.125	10886	182.2	0.0225	76.1	

Table IV-2. Summary of Test Data for Phase II (LH_2) Continued

Test No.	Axial Clearance, in.	Blade Height, in.	Shaft Speed, rpm	Flow Rate, gpm	Flow Coeff.	Reynolds No. (10^6)	Remarks
9.06	0.073	0.125	10899	107.6	0.0251	39.7	
9.07	0.073	0.125	13007	235.4	0.0274	77.0	
9.08	0.073	0.125	12982	199.4	0.0213	87.3	
9.09	0.073	0.125	12996	121.1	0.0193	57.8	
10.01	0.073	0.125	8941	282.0	0.0341	76.4	Bladed Disk, 24 Blades
10.02	0.073	0.125	8947	217.6	0.0268	74.5	
10.03	0.073	0.125	8973	94.5	0.0126	65.8	Tip Blockage Z = 0.150 in.
10.04	0.073	0.125	10980	256.9	0.0258	92.4	
10.05	0.173	0.125	10993	217.4	0.0221	90.6	
10.06	0.073	0.125	11006	128.1	0.0137	83.6	
10.07	0.073	0.125	12099	197.8	0.0187	99.2	
10.08	0.073	0.125	13045	272.5	0.0234	108.2	
10.09	0.073	0.125	13145	239.5	0.0209	107.1	
10.10	0.073	0.125	13051	226.0	0.0199	105.0	
10.11	0.073	0.125	13066	183.2	0.0165	101.6	
10.12	0.073	0.125	14735	235.5	0.0189	116.6	
10.13	0.073	0.125	15619	233.8	0.0179	121.7	
11.01	F=0.156	0.125	9798	140.0	F=0.0126	F=72.3	Bladed Disk, 24 Blades
	R=0.135	0.125			R=0.0138	R=71.8	
11.02	R=0.135	0.125	9796	206.0	F=0.0177	F=76.5	
	R=0.135	0.125			R=0.0195	R=75.3	
11.03	R=0.135	0.125	9777	240.0	F=0.0203	F=78.0	Front and Rear Clearance Not Equalized (F-Front, R-Rear)
	R=0.135	0.125			R=0.0222	R=77.0	
11.04	R=0.135	0.125	12131	186.0	F=0.0143	F=85.4	
	R=0.135	0.125			R=0.0159	R=83.4	
11.05	R=0.135	0.125	12122	222.0	F=0.0165	F=88.6	
	R=0.135	0.125			R=0.0181	R=87.6	
11.06	R=0.135	0.125	12107	234.0	F=0.0173	F=89.4	
	R=0.135	0.125			R=0.0189	R=88.5	
11.07	R=0.135	0.125	13997	240.0	F=0.0164	F=96.6	
	R=0.135	0.125			R=0.0179	R=95.8	
11.08	R=0.135	0.125	13547	220.0	F=0.0155	F=93.9	
	R=0.135	0.125			R=0.0170	R=92.2	
11.09	R=0.135	0.125	13593	210.0	F=0.0149	F=93.1	
					R=0.0164	R=91.3	
12.01	0.073	0.125	8938	190.0	0.0233	76.1	Bladed Disk, 24 Blades
12.02	0.073	0.125	8934	255.0	0.0310	77.3	
12.03	0.073	0.125	10952	88.9	0.0097	85.0	Tip Blockage Z = 0.100 in.
12.04	0.073	0.125	9069	98.6	0.0125	71.5	
12.05	0.073	0.125	9050	95.1	0.0122	70.9	

Bearing failure aborted test

Table IV-2. Summary of Test Data for Phase II (LH_2) Continued

Test No.	Axial Clearance, in.	Blade Height, in.	Shaft Speed, rpm	Flow Rate, gpm	Flow Coeff.	Reynolds No. (10^6)	Remarks
13.01	0.074	0.125	9427	316.2	0.0362	81.8	Bladed Disk, 12 Blades
13.02	0.074	0.125	9404	255.4	0.0298	79.9	
13.03	0.074	0.125	9476	192.6	0.0232	76.9	
13.04	0.074	0.125	11189	298.8	0.0298	93.8	
13.05	0.074	0.125	11133	248.1	0.0255	90.7	
13.06	0.074	0.125	11173	166.1	0.0187	81.8	
13.07	0.074	0.125	13212	261.4	0.0240	102.1	
13.08	0.074	0.125	13054	231.5	0.0221	97.6	
13.09	0.074	0.125	13234	209.3	0.0204	95.7	
14.01	0.075	0.125	8996	270.0	0.0320	78.5	Bladed Disk, 6 Blades
14.02	0.075	0.125	9001	222.0	0.0267	77.1	
14.03	0.075	0.125	9012	147.1	0.0184	73.3	
14.04	0.075	0.125	10993	266.0	0.0264	93.5	
14.05	0.075	0.125	11000	201.4	0.0207	90.0	
14.06	0.075	0.125	10970	154.4	0.0166	85.7	
14.07	0.075	0.125	12944	209.5	0.0192	101.4	
14.08	0.075	0.125	12955	176.7	0.0167	98.0	
14.09	0.075	0.125	12952	150.8	0.0147	94.8	
15.01	0.072	0.250	9270	133.6	0.0113	68.0	Bladed Disk, 24 Blades
15.02	0.072	0.250	9213	205.5	0.0157	75.4	
15.03	0.072	0.250	9200	255.0	0.0191	77.5	
15.04	0.072	0.250	11251	194.0	0.0132	84.9	
15.05	0.072	0.250	11223	255.6	0.0164	91.6	
15.06	0.072	0.250	11174	254.8	0.0163	90.5	
15.07	0.072	0.250	12984	283.3	0.0140	97.0	
15.08	0.072	0.250	12949	278.8	0.0160	101.3	
15.09	0.072	0.250	12991	303.2	0.0170	103.7	
16.01	0.037	0.250	9230	174.3	0.0154	72.2	Bladed Disk, 24 Blades
16.02	0.037	0.250	9231	213.6	0.0182	77.1	
16.03	0.037	0.250	9232	256.0	0.0213	78.5	
16.04	0.037	0.250	11277	167.3	0.0128	82.7	
16.05	0.037	0.250	11293	228.3	0.0162	92.3	
16.06	0.037	0.250	11295	275.9	0.0191	94.4	
16.07	0.037	0.250	13327	218.4	0.0143	99.3	
16.08	0.037	0.250	13345	256.2	0.0159	103.0	
16.09	0.037	0.250	13300	296.1	0.0179	105.0	

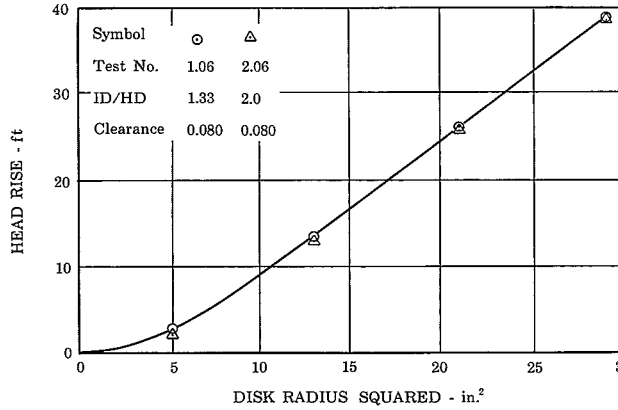

Figure IV-1. Radial Head Distribution for Smooth Disk with Inlet Hub in Water - Radially Outward Flow FD 10999(U)

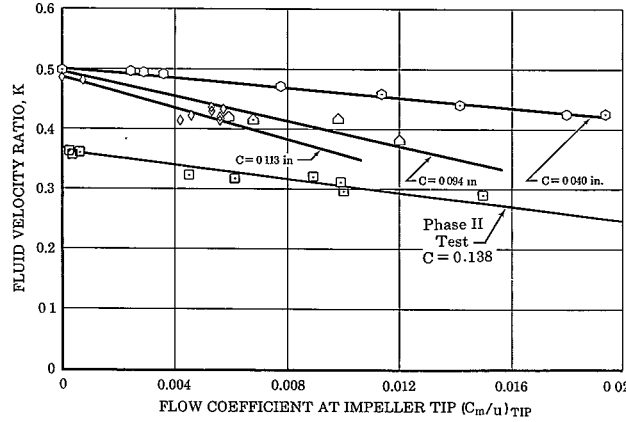

Figure IV-2. Fluid Velocity Ratio vs Flow Coefficient for Smooth Disk in Water - Radially Outward Flow FD 10999(L)

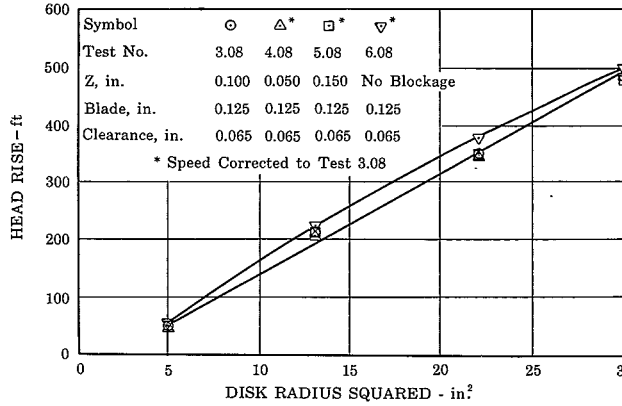

(a) Radially Outward Flow

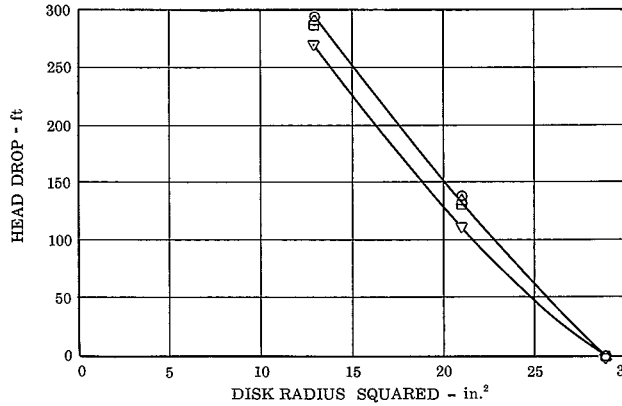

(b) Radially Inward Flow

Figure IV-3. Radial Head Distribution for Bladed Disk with Tip Blockage in Water FD 10998

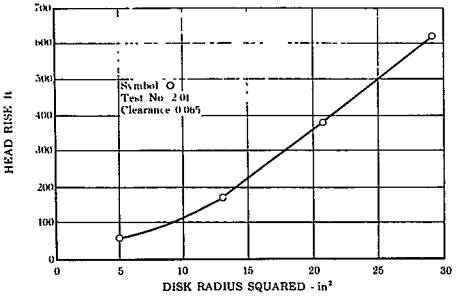

(a) Smooth Disk
Outward Flow

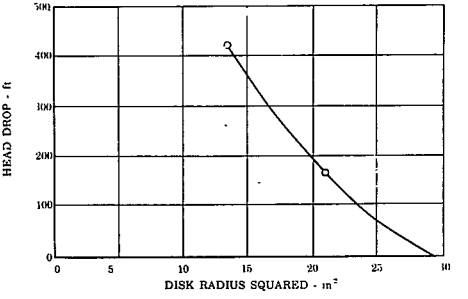

(b) Smooth Disk
Inward Flow

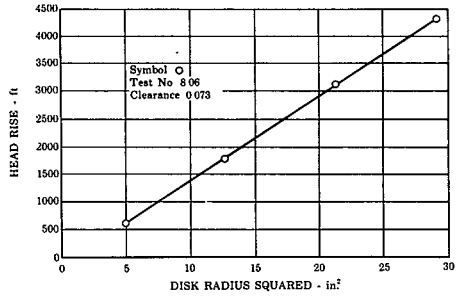

(c) Bladed Disk, 24 Blades, 0.125 in. High
Outward Flow

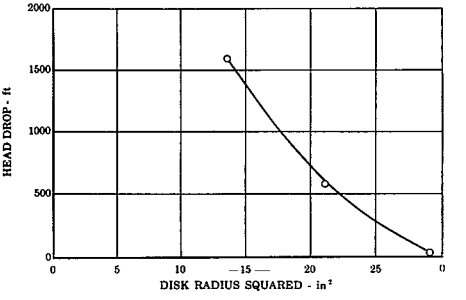

(d) Bladed Disk, 24 Blades, 0.125 in. High
Inward Flow

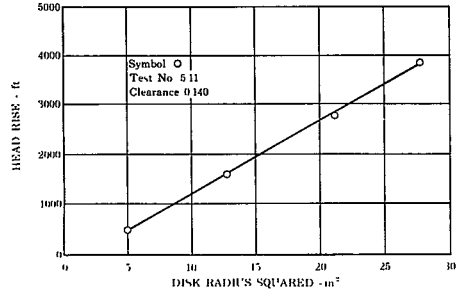

(e) Bladed Disk, 24 Blades, 0 250 in. High
Outward Flow

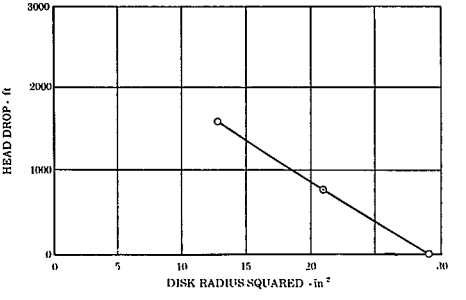

(f) Bladed Disk, 24 Blades, 0.250 in. High
Inward Flow

Figure IV-4. Typical Head Distribution for Smooth and Bladed Disks in Liquid Hydrogen FD 11015

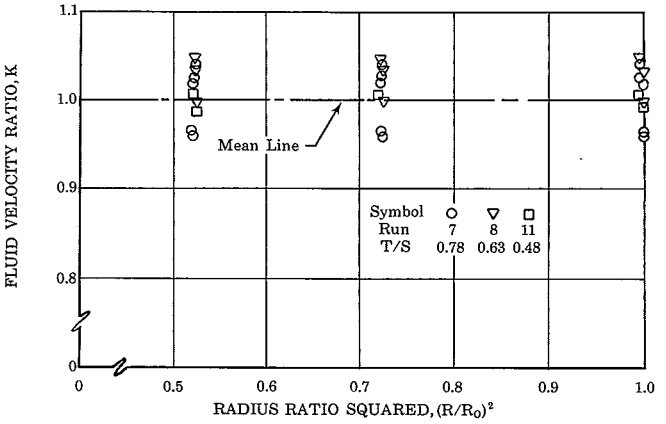

(a) T = 0.125

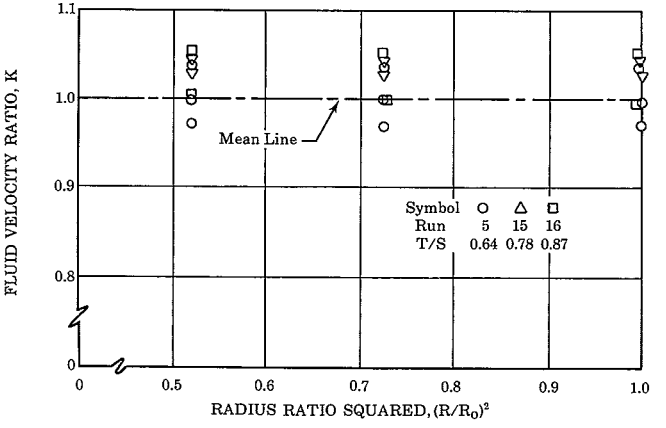

(b) T = 0.250

Figure IV-5. Fluid Velocity Ratio vs Radius Ratio Squared for Bladed Disk in Liquid Hydrogen - Radially Outward Flow FD 10985

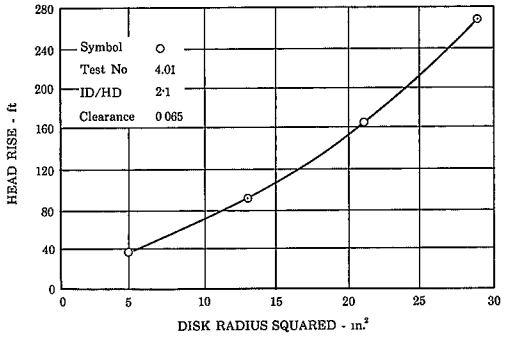

(a) Radially Outward Flow

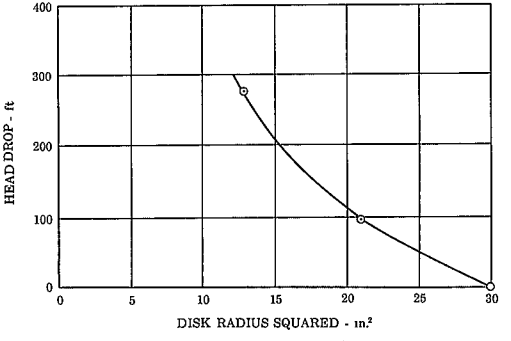

(b) Radially Inward Flow

Figure IV-6. Radial Head Distribution for Smooth Disk with Hub in Liquid Hydrogen FD 11000(U)

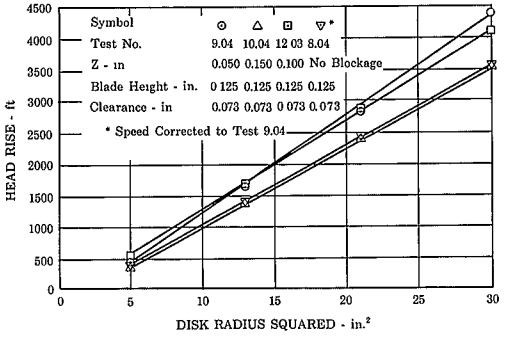

(a) Radially Outward Flow

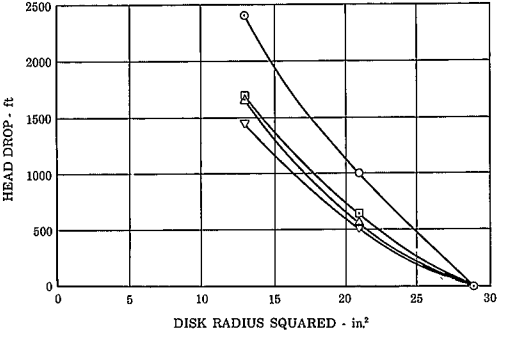

(b) Radially Inward Flow

Figure IV-7. Radial Head Distribution for Bladed Disk with Tip Blockage in Liquid Hydrogen FD 11000(L)

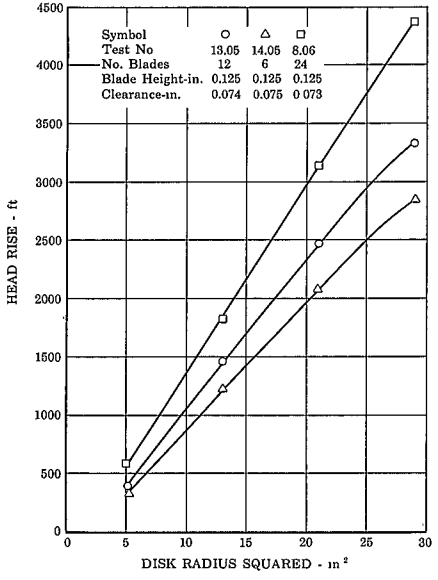

a) Radially Outward Flow

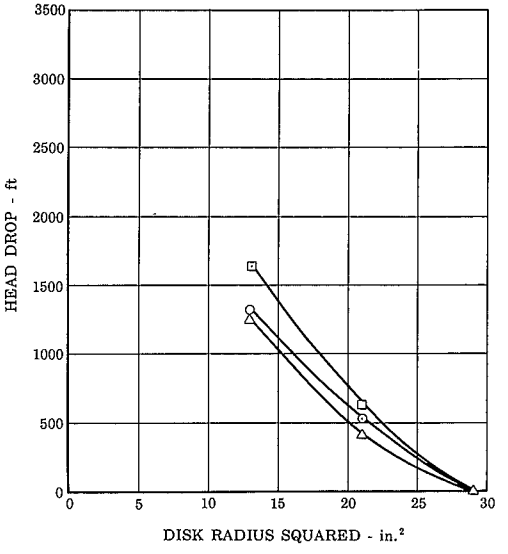

b) Radially Inward Flow

Figure IV-8. Radial Head Distribution for Bladed Disk with Varying Number of Blades in Liquid Hydrogen

FD 10991(L)
FD 10992(R)

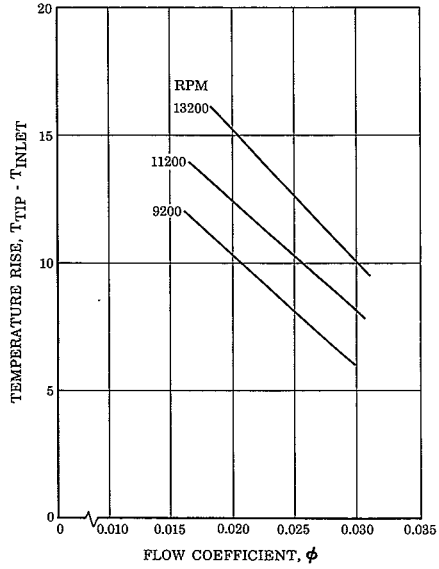

Figure IV-9. Typical Temperature Rise vs Flow Coefficient for Bladed Disk in Liquid Hydrogen FD 10990

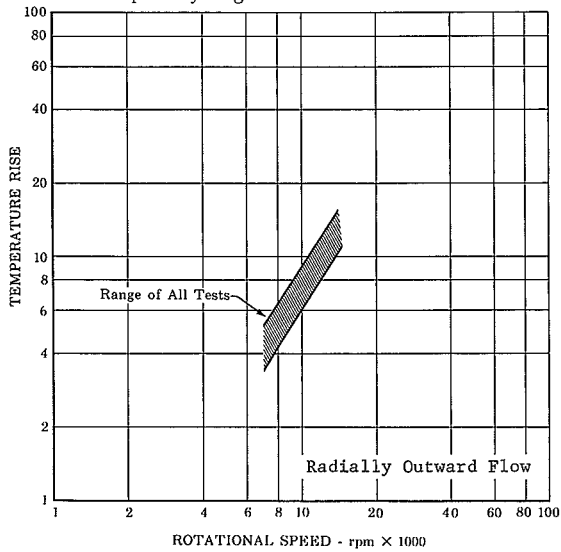

Figure IV-10. Temperature Rise vs Rotational Speed for Bladed Disk in Liquid Hydrogen FD 10988

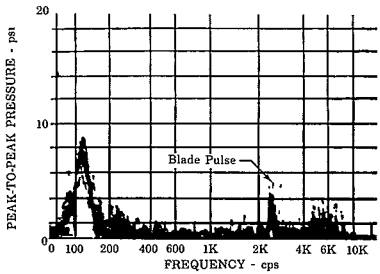

(a) Test 5.08 24 Blades
T = 0.250 C = 0.140

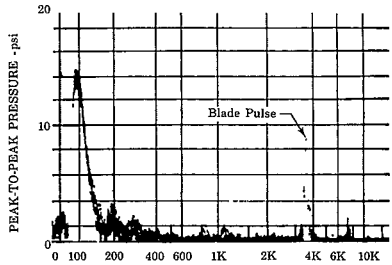

(b) Run 8.03 24 Blades
T = 0.125 C=0.073

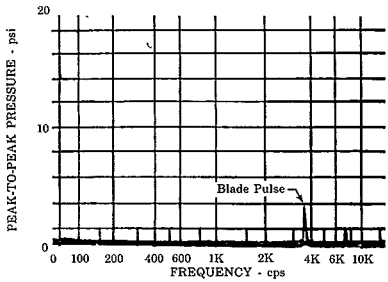

(c) Test 9.02 24 Blades
T = 0.125 C = 0.073
z = 0.050

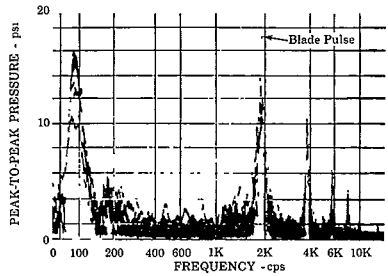

(d) Test 13.03 12 Blades
T = 0.125 C = 0.073

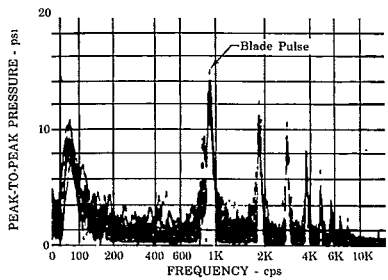

(e) Test 14.03 6 Blades
T = 0.125 C = 0.075

Figure IV-11. Panoramic Wave Analysis for Bladed Disk in Liquid Hydrogen - $(R/R_o)^2$ = 0.724

FD 11002

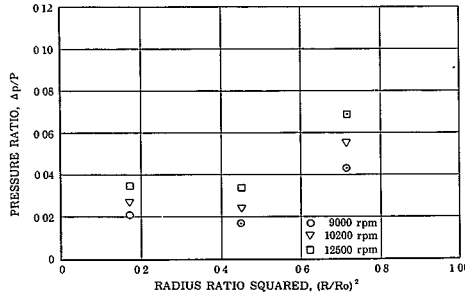

(a) 24 Blades T = 0.125 C = 0.035

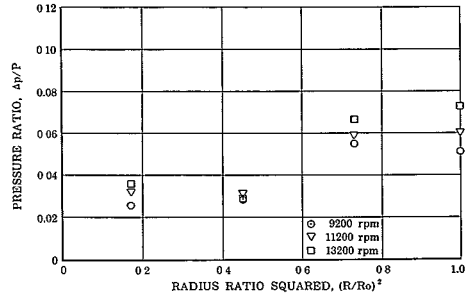

(b) 24 Blades T = 0 125 C = 0.074

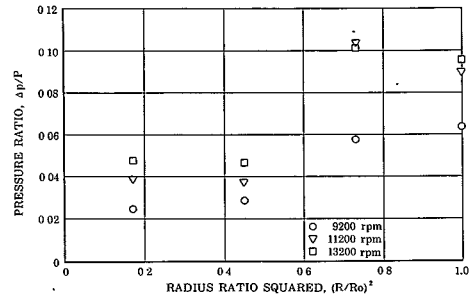

(c) 24 Blades T = 0.125 C = 0.156

Figure IV-12. Blade Pressure Loading vs Radius Ratio Squared in Liquid Hydrogen FD 11001

SECTION V
APPLICATION OF RESULTS

A. GENERAL

The results of the experimental program have been used to develop methods for predicting the pressure distribution generated by low flow radial impellers within the range of variables tested. The prediction methods involve a series of regression equations for calculating fluid angular velocity ratio, each equation being applicable to a given configuration and working fluid. The equations derived from the water test results are applicable to any incompressible fluid with a Reynolds number greater than 10^6, while the equations for liquid hydrogen are applicable only to liquid hydrogen because of the unique properties of this cryogenic fluid.

The prediction methods are based on a limited amount of data in some cases and additional testing is recommended to confirm basic trends established to date and investigate several areas as yet unexplored.

B. DERIVATION OF K VALUE

The pressure distribution along the face of a low flow radial impeller can be described by use of the forced vortex equation,

$$H_2 - H_1 = P_2/\gamma_2 - P_1/\gamma_2 = \beta^2/2g\ (R_2^2 - R_1^2) \qquad (3)$$

if the fluid angular velocity, β, in the flow passage is known. For convenience the relationship,

$$\beta = K\omega \qquad (4)$$

is used to provide a dimensionless fluid velocity ratio, K, in place of β, so that equation 3 becomes,

$$H_2 - H_1 = (K^2\omega^2/2g)\ (R_2^2 - R_1^2) \qquad (5)$$

For a forced vortex, K remains constant with respect to radial span and varies only as a function of geometry and flow rate. In other vortex modes (such as free or superforced or any form in between these extremes) K varies as a function of radial span as well as geometry and flow rate. Therefore, by determining the effect on K of various configurations and flow conditions the forced vortex equation in the form

$$P_2 - P_1 = (\gamma K^2\omega^2/2g)\ (R_2^2 - R_1^2) \qquad (6)$$

can be used to calculate pressure distribution.

As discussed in Section IV, the data from the experimental program has been used to formulate regression equations for K for each configuration and test fluid that reflect the dependence of K on each variable. The calculation procedure for the pressure distribution is as follows:

1. Forced vortex: The value of K is determined from the applicable regression equation and, since K is constant with respect to radial span, the ΔP across the face of the rotor can be readily calculated using the forced vortex equation.

2. Other vortex modes:

   a. The rotor is divided into small radial increments and the value of K determined from the applicable regression equation at the average radius of each increment.

   b. ΔP is then calculated for each radial increment across the face of the rotor from the forced vortex equation.

C. DETERMINATION OF K VALUE

The following equations were derived from the statistical fit of all test data for the configurations investigated and reflect the dependence of K on each variable. The maximum (MPE) and average (APE) percent of error of the analytical expression with respect to the test data is presented with each equation. The equations for the smooth disk in water are based on data from tests in Phase I and II.

1. Smooth Disk - Outward Flow with Water

$$K = 0.578 - 4.11\,\phi - 1.67C \qquad (7)$$

MPE = 4.5%

APE = 2.0%

Figure V-1a shows a plot of K vs flow coefficient for three clearances. As can be seen from equation 7, K is independent of radius indicating the existance of a forced vortex. It should also be noted that K is a linear function of flow coefficient and clearance. Figure V-2a is a cross-plot of K vs clearance for three flow coefficients.

2. Smooth Disk - Inward Flow with Water

$$K = 0.3865 + 95.3\,\phi^2 - 12.6\,\phi\left(\frac{R}{R_o}\right)^2 - 9.17 \times 10^5\,\phi\left(\frac{C}{R_o}\right)^3 + 2.78\left(\frac{R}{R_o}\right)^2\left(\frac{C}{R_o}\right) - 2.75 \times 10^3\left(\frac{R}{R_o}\right)^4\left(\frac{C}{R_o}\right)^2 + 6.51 \times 10^4\left(\frac{R}{R_o}\right)^6\left(\frac{C}{R_o}\right)^3 + 2.13\,\phi^{0.5} - 6.59\left(\frac{C}{R_o}\right) \quad (8)$$

MPE = 28.6%

APE = 4.92%

In the inward flowing case K is a function of R, C, and ϕ indicating a vortex mode other than forced. Figure V-1b is a plot of K vs flow coefficient for three clearances at $(R/R_o)^2 = 1$ or at the tip of the disk. Figure V-2b shows curves of K vs clearance for three values of ϕ and shows the decrease in the effect of flow coefficient with a reduction in clearance. Figures V-3a and V-3b are cross-plots of K vs $(R/R_o)^2$ with lines of constant ϕ and C/R_o, respectively.

3. Smooth Disk - Outward Flow with Hydrogen

$$K = 0.906 + 0.012\,\phi\left(\frac{C}{R_o}\right)^{-1.0} - 5.355\,\phi - 51.11\left(\frac{C}{R_o}\right) + 1295.3\left(\frac{C}{R_o}\right)^2 \quad (9)$$

MPE = 29.2%

APE = 5.54%

As in the case of Equation 7 (smooth disk - outward flow with water) a forced vortex exists with liquid hydrogen. But unlike Equation 7, K is not a linear function of clearance and flow coefficient. Figure V-1c presents a set of curves of K vs ϕ produced by Equation 9. Figure V-2c is a plot of K vs clearance for various flow coefficients which shows graphically the nonlinearity of K with clearances.

4. Smooth Disk - Inward Flow with Hydrogen

$$K = 0.18\ \phi^{0.016\left(\frac{R}{R_o}\right) - 1.434\ C - 0.233} \qquad (10)$$

MPE = 4.12%

APE = 1.69%

For inward flow with hydrogen K is a function of R, ϕ, and C. It can be seen from the equation and the curves of figure V-1d that ϕ has a very slight effect on K and can be considered negligible at values above 0.010. Figure V-2d is a cross-plot of the curves from figure V-1d showing the change in K with clearance. Figures V-3c and V-3d are cross-plots of K vs $(R/R_o)^2$ with lines of constant ϕ and C/R_o, respectively.

5. Bladed Disk - Outward Flow with Hydrogen

K = 1.0 and is independent of all variables.

6. Bladed Disk (0.250 Inch Blades) - Inward Flow with Hydrogen

$$K = 0.8819 + 1.24\left(\frac{R}{R_o}\right)^2 - 1.943\left(\frac{R}{R_o}\right)^4 + 841.0\left(\frac{R}{R_o}\right)^6 + 4.06\ T/S - 2.41\ (T/S)^2 - 23.94\left(\frac{R}{R_o}\right)^2 \phi + 1283.1\left(\frac{R}{R_o}\right)^4 \phi^2 - 1.985\left(\frac{R}{R_o}\right)^6 \phi^3 \qquad (11)$$

MPE = 14.37%

APE = 2.28%

K is a function of R, T/S and ϕ for the 0.250 inch blade disk. Figures V-4d, V-4e, and V-4f show curves of K vs $(R/R_o)^2$ for 3 values of ϕ at T/S ratios of 0.8, 0.6, and 0.4, respectively. These curves show the magnitude of the effect of each variable on K. Figure V-5a is a plot of K vs T/S for a ϕ of 0.0195 and $(R/R_o)^2$ of 0.793. Also shown are data points from three tests.

7. Bladed Disk - (0.125 Inch Blades) - Inward Flow with Hydrogen

$$K = -2.511 + 0.495\left(\frac{R}{R_o}\right)^2 + 103.4\,\phi - 726.9\,\phi^2 + 0.26\,T/S - 55.0\left(\frac{R}{R_o}\right)^2\phi + 405.0\left(\frac{R}{R_o}\right)^4\phi^2 + 0.045^{-1} - 0.00026\,\phi^{-2} + 0.069\left(\frac{R}{R_o}\right)^{-1} \quad (12)$$

MPE = 11.92%

APE = 2.11%

As was the case with the 0.250 inch blades K for the 0.125 inch blades is a function of R, T/S and ϕ. Figures V-4a, V-4b, V-4c, show curves of K vs $(R/R_o)^2$ for 3 values of ϕ at different T/S values. Unlike the 0.250 inch blade results ϕ and $(R/R_o)^2$ have a large effect on K while the effect of T/S is slight. Figure V-5b shows a curve from the regression equation with data points from three tests plotted as K vs T/S for a ϕ of 0.022 and $(R/R_o)^2$ of 0.793.

8. End Effects

Regression equations have not been formulated to define the effects on K of changes to the inlet and discharge geometry due to the limited amount of data available. The results of the investigation of end effects are presented in curve form and are discussed in the following paragraphs:

a. Smooth Disk with Inlet Hub-Water

As discussed in Section IV the effect on K of adding an inlet hub to the smooth disk was investigated for two inlet-to-hub diameter ratios, 2.0 and 1.33. The results are shown in figure V-6a, which presents a curve of K vs ϕ at a clearance of 0.080 in. produced from Equation 7 (smooth disk outward flow) and a curve showing the data from the ID/HD = 2.0 hub tests at the same clearance. As evidenced by the curve the addition of a hub results in a significant reduction in K. The reason for these

somewhat unexpected results are as yet unexplained but other investigators such as Daily, et al,† have reported observing a similar phenomena in going from a cylindrical hub to a smooth contoured hub. A comparison of the head rise at each radial station between the tests with and without an inlet hub revealed an increase in head rise at the inlet to the impeller with a hub as would be expected but the slope of the $\Delta H - R^2$ curve beyond the inlet is reduced so that the overall head rise is less than in the case without a hub. Results were the same for both ID/HD ratios. As stated previously additional testing is required to determine if this effect and its magnitude are the same at other clearances.

b. Smooth Disk with Inlet Hub - Hydrogen

Figure V-6b shows a curve of K vs ϕ for outward flow on a smooth disk generated by Equation 9 and a plot of the data from a test with an inlet hub. As can be seen by comparing figure V-6b with figure V-6a, the addition of a hub had a directly opposite effect in hydrogen than in water, that is, the hub caused an increase in K value rather than a decrease. An explanation of these results would require a thorough investigation into the flow characteristics, i.e., turbulence, recirculation, etc. of each configuration and test fluid.

c. Bladed Disk with Tip Blockage - Water

The addition of blockage or overhang at the tip of the bladed impeller changed the vortex mode, creating a forced vortex and making K independent of radius. Figure V-7 shows a curve from the regression equation for a bladed disk with outward flow developed in the Phase I program,

$$K = 0.951 - 0.282\left(\frac{R}{R_o}\right) + 0.2137\ (T/S) + 0.175\ (T) \qquad (13)$$

and a curve from one of the tip blockage tests showing K to be constant with radius. All three tip blockage clearances tested produced the same

† Daily, J. W., W. D. Ernst, V. V. Asbedian, "Enclosed Rotating Disks with Superposed Throughflow," M.I.T. Department of Civil Engineering, Hydrodynamics Laboratory Report No. 64, April 1964.

results. It would appear then that for a bladed disk with tip blockage the R/R_o factor could be dropped from the above equation. However, the tip blockage effect has been investigated at only one value of T/S at one blade height and additional tests should be conducted to confirm this effect.

d. Bladed Disk with Tip Blockage - Hydrogen

Tip blockage on the bladed disk in liquid hydrogen had no effect on K as it remained constant and equal to unity.

D. LIMITATIONS OF THE PREDICTION SYSTEM

The formulas derived for K in this program and their application to a pressure prediction system are limited as follows:

1. To the range of each variable tested, as listed below

Configuration and Test Fluid	Limits ϕ	C	Rey No. ($X10^6$)
Smooth Disk			
Water	0.000 - 0.035	0.040 - 0.138	6.87 - 22.5
Hydrogen	0.004 - 0.123	0.024 - 0.138	77.2 - 123.0
Bladed Disk			
Water	0.000 - 0.024	0.020 - 0.125	3.8 - 27.9
Hydrogen	0.010 - 0.046	0.035 - 0.156	37.3 - 121.7

2. To the fluids tested. The equations based on the water tests are considered applicable to any incompressible fluid within the range of Reynolds numbers tested. The liquid hydrogen equations are limited to use in a hydrogen application only.

Figure V-1. Fluid Velocity Ratio vs Flow Coefficient for Smooth Disk

(a) Water
Outward Flow

(b) Water
Inward Flow

(c) Liquid Hydrogen
Outward Flow

(d) Liquid Hydrogen
Inward Flow

Figure V-2. Fluid Velocity Ratio vs Disk-to-Housing Clearance for Smooth Disk

FD 10982

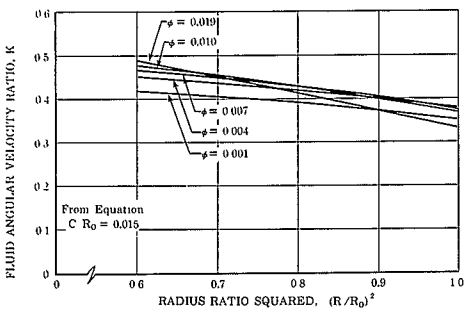

(a) In Water with Constant ϕ

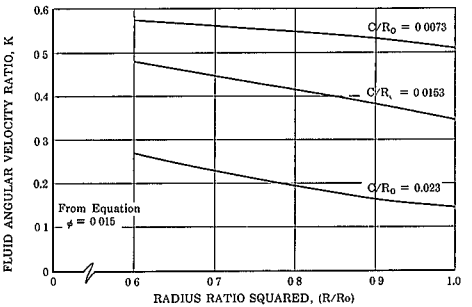

(b) In Water with Constant C/R_o

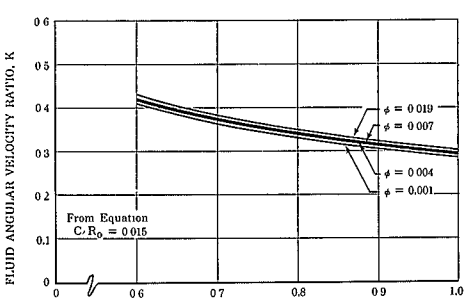

(c) In Liquid Hydrogen with Constant ϕ

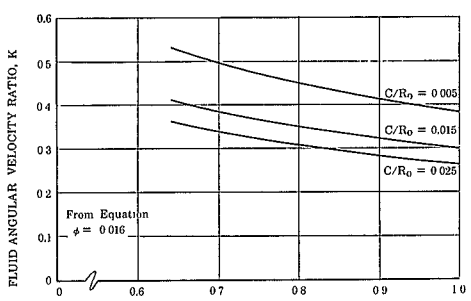

(d) In Liquid Hydqrogen with Constant C/R_o

Figure V-3. Fluid Velocity Ratio vs Radius Ratio Squared for Smooth Disk - Radially Inward Flow FD 10986

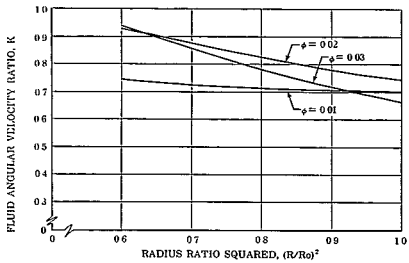

(a) T = 0.125, T/S = 0.8

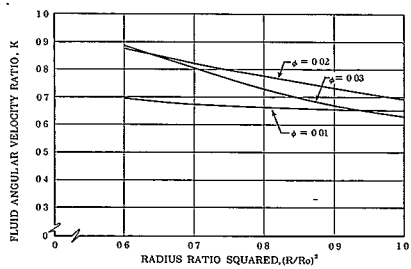

(b) T =0.125, T/S = 0 6

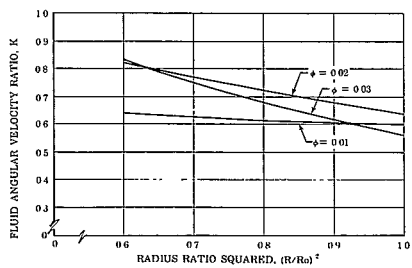

(c) T =0 125, T/S = 0 4

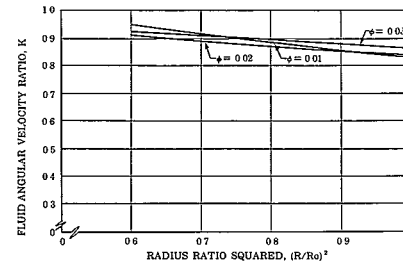

(d) T = 0 250, T/S = 0 8

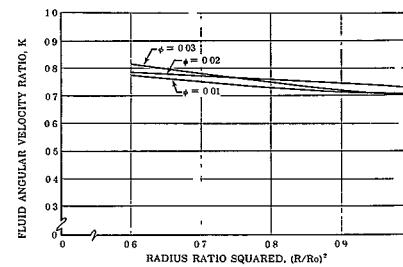

(e) T = 0 250, T/S = 0.6

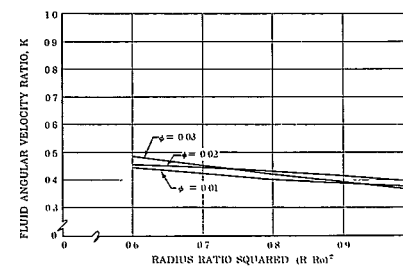

(f) T = 0 250, T/S = 0.4

Figure V-4. Fluid Velocity Ratio vs Radius Ratio Squared for Bladed Disk in Liquid Hydrogen - Radially Inward Flow

FD 11003

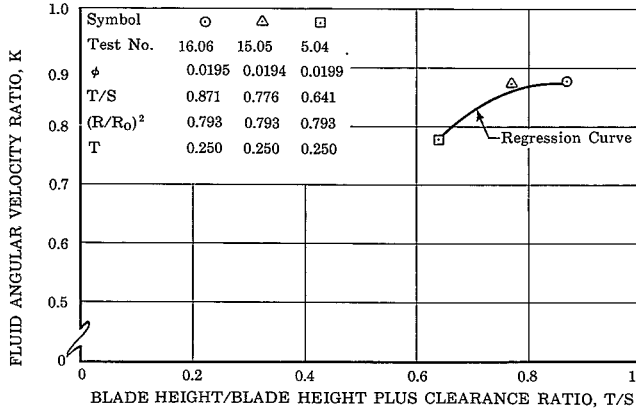

(a) T = 0.250

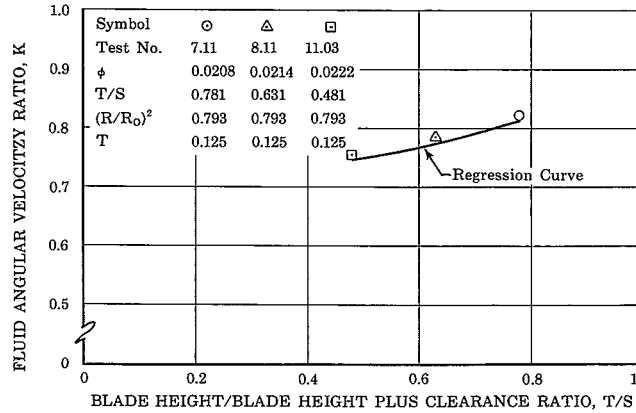

(b) T = 0.125

Figure V-5. Fluid Velocity Ratio vs Blade Height/ Blade Height Plus Clearance for Bladed Disk in Liquid Hydrogen - Radially Inward Flow FD 10983

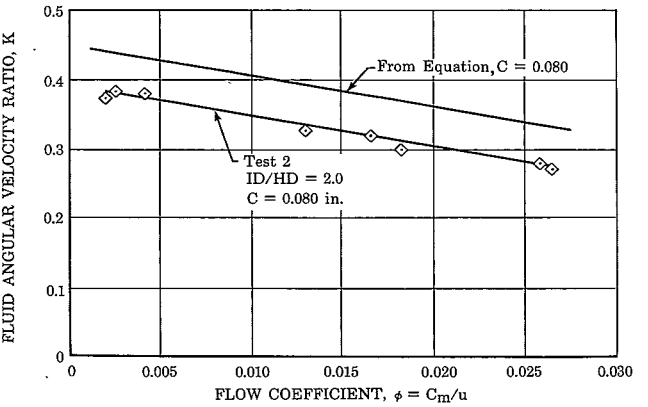

(a) For Water

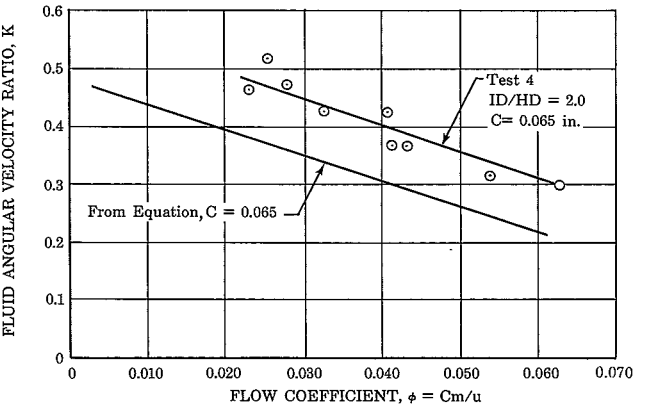

(b) For Liquid Hydrogen

Figure V-6. Fluid Velocity Ratio vs Flow Coefficient FD 10981
for Smooth Disk with Inlet Hub - Radially
Outward Flow

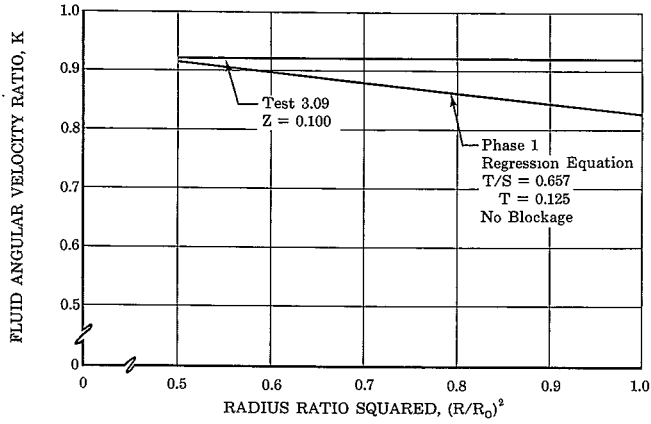

Figure V-7. Fluid Velocity Ratio vs Radius Ratio Squared for Bladed Disk for Bladed Disk with Tip Blockage in Water Radially Outward Flow FD 10979

SECTION VI
CONCLUSIONS

1. A comparison of the results of the water and liquid hydrogen tests revealed several major differences, the most significant of which are listed below:

   a. Smooth Disk (outward flow) - (1) The change in fluid velocity ratio, K, with clearance is linear in water and nonlinear in hydrogen. (2) The addition of an inlet hub reduced the K value in water and increased K in hydrogen.

   b. Bladed Disk (outward flow) - K was found to be constant and equal to unity for all cases tested in hydrogen but varied as a function of R/R_o, T/S, and T in water.

2. The fluid velocity ratio, K, and therefore the pressure distribution for the smooth disk in hydrogen was found to be dependent on flow coefficient and clearance for radially outward flow,

$$K = f(C, \phi)$$ (See figure V-1c.)

and for the radially inward flow,

$$K = f(R/R_o, C, \phi)$$ (See figure V-1d.)

3. For the bladed disk, K was found to be equal to unity and independent of all variables, within the ranges tested, for radially outward flow. A reduction from 24 to 12 or 6 blades had no effect on K.

4. In the case of the bladed disk with radially inward flow K was found to be dependent on flow coefficient, T, T/S and R/R_o,

$$K = f(\phi, T, T/S, R/R_o)$$ (See figure V-4 and V-5.)

5. As mentioned in item 1 above, the addition of an inlet hub to the smooth disk had directly opposite results in liquid hydrogen and water. The hub tests were conducted at only one clearance and additional tests are required to determine whether or not this effect and its magnitude are constant with clearance.

6. Impeller tip blockage on the bladed disk in liquid hydrogen had no effect on K, which remained constant and equal to unity as it was without blockage. In the case of water, on the other hand, the tip blockage raised the value of K and made it independent of R/R_o, (see figure V-7).

Additional tests are required to determine the effect of tip blockage clearance at other values of S (blade height plus blade to housing clearance).

7. The results of the smooth disk tests of Phase II, both in water and liquid hydrogen, do not agree with the findings of other investigators such as Daily and Nece (Reference 3), who have found that at a zero or shutoff flow condition in the channel between a stationary housing and a smooth rotating disk the fluid velocity ratio K is approximately 0.5 for clearances below 0.200 in. This experience plus a scarcity of data resulted in the Phase I smooth disk test results being plotted (K vs ϕ) as a family of curves for varying clearance fanning out from a common apex at a K value of approximately 0.5, (see figure IV-2). The water tests in Phase II gave indications that the lines of constant clearance do not converge at K = 0.5 but are actually parallel (figure V-1a) and that the slope of a curve of K vs clearance (figure V-2a) is quite steep. Subsequent tests in liquid hydrogen confirmed these results (figure V-1c).

8. The high response pressure data from the bladed disk tests in liquid hydrogen failed to provide a fixed relationship between the pressure pulse across the blade and pressure, speed or flow rate. Therefore, it is not possible at this time to develop an equation for predicting blade loading. It is possible, however, that further testing over a wider range of operating conditions may establish trends that would be useful in formulating a prediction system.

SECTION VII
REFERENCES

1. PWA FR-952 - Final report on Phase I of Contract NAS8-5442 "Investigation of Pressure Prediction Methods for Radial Flow Impellers," dated 13 April 1964.

2. Daily, J. W. and R. E. Nece, "Chamber Dimension Effects on Induced Flow and Frictional Resistance of Enclosed Rotating Disks," ASME Transactions, Journal of Basic Engineering, March 1960, pp 217 - 232.

3. Daily, J. W., W. D. Ernst, V. V. Asbedian, "Enclosed Rotating Disks with Superposed Throughflow," M.I.T. Department of Civil Engineering, Hydrodynamics Laboratory Report No. 64, April 1964.

4. Smooth Disk - Inward Flow with Hydrogen

$$K = 0.18\ \phi^{0.016}\left(\frac{R}{R_o}\right) - 1.434\ C - 0.233 \qquad (10)$$

MPE = 4.12%

APE = 1.69%

For inward flow with hydrogen K is a function of R, ϕ, and C. It can be seen from the equation and the curves of figure V-1d that ϕ has a very slight effect on K and can be considered negligible at values above 0.010. Figure V-2d is a cross-plot of the curves from figure V-1d showing the change in K with clearance. Figures V-3c and V-3d are cross-plots of K vs $(R/R_o)^2$ with lines of constant ϕ and C/R_o, respectively.

5. Bladed Disk - Outward Flow with Hydrogen

K = 1.0 and is independent of all variables.

6. Bladed Disk (0.250 Inch Blades) - Inward Flow with Hydrogen

$$K = 0.8819 + 1.24\left(\frac{R}{R_o}\right)^2 - 1.943\left(\frac{R}{R_o}\right)^4 + 841.0\left(\frac{R}{R_o}\right)^6 + 4.06\ T/S - 2.41\ (T/S)^2 - 23.94\left(\frac{R}{R_o}\right)^2\phi + 1283.1\left(\frac{R}{R_o}\right)^4\phi^2 - 1.985 \times 10^4\left(\frac{R}{R_o}\right)^6\phi^3 \qquad (11)$$

MPE = 14.37%

APE = 2.28%

K is a function of R, T/S and ϕ for the 0.250 inch blade disk. Figures V-4d, V-4e, and V-4f show curves of K vs $(R/R_o)^2$ for 3 values of ϕ at T/S ratios of 0.8, 0.6, and 0.4, respectively. These curves show the magnitude of the effect of each variable on K. Figure V-5a is a plot of K vs T/S for a ϕ of 0.0195 and $(R/R_o)^2$ of 0.793. Also shown are data points from three tests.